Photoacoustics 18 (2020) 100171

Contents lists available at ScienceDirect

Photoacoustics

journal homepage: www.elsevier.com/locate/pacs

Photoacoustic and fluorescence lifetime imaging of diatoms

Julijana Cvjetinovic[a,*], Alexey I. Salimon[b], Marina V. Novoselova[a], Philipp V. Sapozhnikov[c], Evgeny A. Shirshin[d,e], Alexey M. Yashchenok[a], Olga Yu. Kalinina[f], Alexander M. Korsunsky[b,g], Dmitry A. Gorin[a,*]

[a] Center for Photonics and Quantum Materials, Skolkovo Institute of Science and Technology, 3 Nobelya Str., Moscow, 121205, Russia
[b] Center for Energy Science and Technology, Skolkovo Institute of Science and Technology, 3 Nobelya Str., Moscow, 121205, Russia
[c] Shirshov Institute of Oceanology of Russian Academy of Sciences, 36 Nakhimovsky Prospekt, Moscow, 117997, Russia
[d] Lomonosov Moscow State University, 1/2 Leninskiye Gory, Moscow, 119991, Russia
[e] Institute of Spectroscopy of the Russian Academy of Sciences, 5 Fizicheskaya Str., Troitsk, Moscow, 108840, Russia
[f] Faculty of Geography, Lomonosov Moscow State University, 1 Leninskiye Gory, Moscow, 119991, Russia
[g] Department of Engineering Science, University of Oxford, Oxford, OX1 3PJ, United Kingdom

ARTICLE INFO

Keywords:
Diatoms
Dynamic light scattering
Absorbance
Fluorescence spectroscopy
Fluorescence lifetime imaging microscopy
Photoacoustic imaging
Scanning electron microscopy

ABSTRACT

Photoacoustic and fluorescent methods are used intensely in biology and medicine. These approaches can also be used to investigate unicellular diatom algae that are extremely important for Earth's ecology. They are enveloped within silica frustules (exoskeletons), which can be used in drug delivery systems. Here, we report for the first time the successful application of photoacoustic (PA) and fluorescent visualization of diatoms. Chlorophyll *a* and *c* and fucoxanthin were found likely to be responsible for the photoacoustic effect in diatoms. The PA signal was obtained from gel drops containing diatoms and was found to increase with the diatom concentration. The fluorescence lifetime of the diatom chromophores ranged from 0.5 to 2 ns. The dynamic light scattering, absorbance, and SEM characterization techniques were also applied. The results were considered in combination to elucidate the nature of the photoacoustic signal. Possible biotechnological applications are proposed for the remote photoacoustic monitoring of algae.

1. Introduction

Photoacoustics is attracting growing scientific and practical interest, because it can characterize tissues, cells, and drug delivery containers for diagnostic purposes and for *in situ* therapy facilitated by plasmonic heating [1–5]. Photoacoustic visualization methods are readily used to collect meaningful acoustic signals from complex biological objects with unprecedented spatial accuracy of detection of their components containing light-absorbing molecules. The excitation of hierarchically finer scale objects—light-absorbing chromophore molecules (melanin, hemoglobin, water, lipid, etc.)—ultimately converts to the vibrations of much bigger, hierarchically larger-scale objects such as cell organelles (e.g. melanosomes) or whole cells (erythrocytes) [1,4]. The flow of energy across hierarchical levels of organization is associated with the changes in the underlying physical phenomena according to size and scale effects [6]. The frequencies of these vibrations, recorded owing to the optically driven acoustic signal, range from 1 MHz to 100 MHz, which is of the same order of magnitude as the eigenfrequencies of capsular mechanical objects having sub- and micrometer sizes [7].

To the best of our knowledge, very limited data [8–10] are available on the photoacoustic studies of single-cell organisms—both prokaryotes (e.g. cyanobacteria) and eukaryotes (e.g. diatoms)—which contain light-absorbing chromophores such as chlorophyll or carotenoids. We believe that photoacoustic visualization of such living objects may have a number of ecological, biotechnological, and biomedical applications, such as the remote and rapid control over microbial cultures and media, cell studies, sanitary control, and aquaculture. The photoacoustic technique is very interesting from the standpoint of observations on diatoms in their natural environments and also during culturing. It is potentially possible to install photoacoustic tools in vessels or in harbor constructions that are used to monitor diatoms in aquatic environments. Owing to laser irradiation and subsequent absorption of light by the diatom chromophores, the photoacoustic method is promising for studying the activity of these objects in their natural environments, as

* Corresponding authors.
E-mail addresses: Julijana.Cvjetinovic@skoltech.ru (J. Cvjetinovic), D.Gorin@skoltech.ru (D.A. Gorin).

https://doi.org/10.1016/j.pacs.2020.100171
Received 21 November 2019; Received in revised form 20 January 2020; Accepted 25 February 2020
Available online 10 March 2020

well as for monitoring their growth in bioreactors or aquaculture installations by means of the imaging of colonies. Moreover, photoacoustic visualization of symbiotic bacteria such as stomach flora or plunge bacteria is likely to be potentially useful in some diagnostic tasks.

To approach the problem from all angles, one should use a combination of spectroscopic methods, such as fluorescence and absorbance spectroscopy, and imaging characterization techniques, namely fluorescence lifetime imaging microscopy and photoacoustic imaging. All these methods are mutually considered in order to understand the origin of photoacoustic signals.

Fluorescence spectroscopy as a highly sensitive technique has been widely used to monitor phytoplankton. Two types of light-harvesting pigments of diatoms are well documented [11–14]: chlorophylls and carotenoids. The predominant form of chlorophyll observed in diatoms is chlorophyll *a*, which absorbs energy in the violet-blue and orange-red regions [12–15]. Unlike many other types of algae, diatoms also contain chlorophyll *c*, which absorbs mostly blue and red light [11–13]. The main carotenoid identified in diatoms is fucoxanthin, which absorbs light in the blue-to-green region of the spectrum [11,13–15]. The optical properties of these objects can be better understood when additionally investigating the fluorescent properties. Absorbance spectroscopy measurements are employed to prove the presence of chlorophylls *a* and *c* and fucoxanthin.

Fluorescence lifetime imaging microscopy is a powerful tool for studying biological structures by measuring the fluorescence decay rate of molecules [16–18]. This technique has recently found use in many applications, because it can provide both information on the location of specific fluorophores and on their local environment [16–19]. As an intrinsic property of a fluorophore, the fluorescence lifetime depends on temperature, pH, concentration, polarity, the presence of fluorescence quenchers, and internal factors that are connected with fluorophore structure [18,19]. Therefore, it is important to understand the state of the fluorophore in diatoms. According to the literature, the fluorescence lifetimes of chlorophyll *a* range from 3.0 to 5.1 ns for an isolated molecule, depending on the polarity of the solvent [20]. In living cells, the lifetime ranges from 0.3 to about 1.5 ns, because a great amount of absorbed energy is used in photochemical reactions [20]. It is well known that diatoms use the mechanism of nonphotochemical quenching of chlorophyll *a* fluorescence to dissipate excess energy and prevent overexcitation of the photosynthetic apparatus [21].

We report the findings of our recent research aimed to fill the lacunae in the photoacoustics of single-cell organisms. Diatoms were chosen for study because of their exceptionally important role in Earth's ecology. Diatom species, which constitute a quarter of Earth's biomass, attract generations of scientists of different specialties owing to their fascinating variety, multifunctionality, and specific mechanical strength of their neatly nanostructured silica frustules [22]. Diatoms are frequently found in freshwater bodies [23] and, as a result, may also be detected in human living tissues (e.g. in kidneys) [23,24]. Moreover, diatom frustules are regarded as possible drug delivery containers [25–31]. We demonstrate that the photoacoustic visualization of diatoms is feasible and discuss the source of the photoacoustic signal, its spatial distribution, and the possible further developments toward practical applications.

2. Materials and methods

2.1. Collection and culturing of diatoms

Benthic diatom species were collected from the tidal zone of Gdansk Bay, Baltic Sea in the area of Zelenogradsk, in early June 2016. The salinity of the interstitial water across the collection sites, as well as the water salinity of the tide pools, was 5 ppt. Samples were collected in the mid-littoral zone during the low tide in the form of strips of sand with a width of 1.5 cm, length up to 15 cm and a depth of 0.7–0.9 cm, by using a 0.5-l polyethylene terephthalate (PET) bottle. Then, the sample container was filled with water from a nearby tide pool. The specimen was not fixed, but it was preserved alive and subsequently delivered to Moscow. The material in the bottle was placed on the windowsill of the laboratory to ensure natural diffuse lighting and an alternating day/night regime. The temperature ranged from 17 to 26 °C, and the material was kept in the same plastic bottle for 3 years. The cap of the bottle was slightly loose so as not to hamper the gas exchange between the internal space of the container and the external environment and accommodate room temperature variation. The water capacity of the sample (water + sand at the bottom of the bottle) was 400 ml. The amount of water evaporated from the sample container was recovered by trickling distilled water down the inner wall of the bottle, once the evaporation achieved more than 5 mm from the initial level. This was done to avoid the fouling diatoms inhabiting the PET bottle close to the water surface being osmotically stressed. During the growth period of the accumulation culture, no minerals were fed.

At the end of June 2016, we observed microscopic colonies of *Karayevia amoena* (*K. amoena)* on the surface of sand grains in the ground sample. Permanent preparations were used to identify the species. The frustules were purified from organic components with concentrated sulfuric acid and were embedded in rosin. The data published by diatoms.org [32] were used to ascertain the taxonomic affiliation of the species.

The macroscopic monocultural colonies of *K. amoena*, appearing as brown spots with ramified edges (diameter, 2–3 mm), were observed on the inner surface of the PET bottle in October 2017. By mid-July 2019, a complete brown coating had already been formed by the colonies on the inner wall of the bottle. As part of this coating, *K. amoena* cells were arranged in a dense one-layer pattern and formed a complex ornamented mosaic.

2.2. Scanning electron microscopy

Scanning electron microscopy (Quattro S, Thermo Fisher Scientific, USA) was used to investigate the appearance, morphology, and dimensions of the diatoms. Before SEM analysis, 20 µl of a stock suspension of *K. amoena* was deposited on a precleaned crystalline silicon substrate and three-stage drying in a vacuum oven (50 °C for 5 h, 80 °C for 3 h, and 100 °C for 1 h) was carried out to eliminate any organic components. Samples were mounted on an aluminum stub by using a double-sided carbon adhesive tape and were analyzed without sputter coating at an accelerating voltage of 2.5–5 kV.

2.3. Dynamic light scattering (DLS) measurements

The size and zeta-potential of *K. amoena* dispersed in water (pH 7) were characterized by dynamic light scattering and microelectrophoresis combined with phase analysis light scattering (M3-PALS), by using a Zetasizer Nano ZS instrument (Malvern Instruments Ltd, UK).

2.4. Fluorescence spectroscopy

Fluorescence spectra were recorded with an Infinite M Nano+ (Tecan Trading AG, Switzerland) dual-mode microplate reader. The stock suspension of *K. amoena* (concentration, 305 cells/µl) was diluted to 152.5, 76.3, 38.1, 19.1, 9.5, 4.8, and 2.4 cells/µl. Two ml of diluted suspensions mixed with agarose gel was poured into a 96-well plate, and the plate was placed into a microplate reader. The samples were excited at 530 nm, and their emission was observed in the red range (620–750 nm).

2.5. Absorbance spectroscopy

The absorbance spectra of *K. amoena* suspensions (concentrations, 305, 152.5, 76.3, 38.1, 19.1, 9.5, 4.8, and 2.4 cells/µl) mixed with

agarose gel were obtained with the Infinite M Nano+ reader in the wavelength range 400–750 nm with a 2-nm wavelength step and a 9-nm bandwidth.

2.6. Fluorescence lifetime imaging microscopy (FLIM) measurements

Fluorescence lifetime imaging microscopy (FLIM) measurements and image processing were done as described before [33], by using a MicroTime 200 STED microscope (PicoQuant GmBH, Germany), a 638-nm laser as the excitation source, and a 690-nm bandpass filter. Measurements were carried out at a pulse rate of 40 MHz, a pulse duration of 40 ps, and a maximum power of 50 µW. Fluorescence lifetime images were acquired in the time domain. The laser beam was focused on diatom cells with a 100 × 1.4 NA oil immersion objective (UplanSApo, Olympus, Japan). According to the dwell time of 0.2 ms with a pixel size of 0.200 µm/px, the total image acquisition time was 40 s for an image size of 400 × 400 pixels—i.e. 80 × 80 µm.

2.7. Photoacoustic measurements

Before measurements, the *K. amoena* stock suspension was removed from the bottom of the plastic bottle and was diluted 1:2 seven times. A 0.1-g portion of agarose (Low type 1-B, A-0576, Sigma-Aldrich, Germany) was mixed with 10 ml of distilled water at 120 °C to obtain agarose gel. The concentration was determined with a hemocytometer (Goryaev's chamber). Different *K. amoena* concentrations (1080, 540, 270, 135, 67.5, 33.8 16.9, and 8.4 cells/µl) were mixed with agarose (3 µl of the suspension plus 7 µl of 1 % melted agarose). *K. amoena*-free agarose and *K. amoena*–agarose mixtures (in descending order of dilutions) were pipetted into a petri dish that was subsequently filled with water and placed in the imaging chamber of an RSOM Explorer P50 setup (iThera Medical GmbH, Germany). The photoacoustic signal of the agarose-gel-embedded *K. amoena* was excited by a Wedge HB frequency-doubled flashlamp-pumped Nd:YAG laser (Bright Solutions, Pavia, Italy) at an excitation wavelength of 532 nm (repetition rate, 1–2 kHz; pulse energy, 200 µJ; pulse length, 2.5 ns). The agarose–diatom samples were scanned over an 11 × 11 × 2.5 mm field of view with a raster step size of 20 µm. The axial and lateral resolution capabilities of the RSOM system were 10 µm and 40 µm, respectively. Induced photoacoustic signals were detected with a custom-made spherically focused $LiNbO_3$ detector (center frequency, 50 MHz; bandwidth, 11–99 MHz; focal diameter, 3 mm; focal distance, 3 mm).

Images were processed with ImageJ software. Values for the volume of 3D objects were obtained by generating a maximum intensity projection (MIP) image, drawing a region of interest (ROI) around the area of the signal, and setting a threshold for the image stack to keep visible only the pixels above a certain signal intensity, thus eliminating the background. The thresholded area was measured by using the ROI manager and Multi Measure function. The mean pixel intensity was found from MIP RGB images by analyzing the color histograms of the images, which show the mean pixel intensity for the red and green channels.

3. Results and discussion

3.1. Scanning electron microscopy

The SEM image in Fig. 1a illustrates a general mosaic of the arrangement of diatom cells in the colony. The close-up images of individual diatom frustules in Fig. 1 illustrate their unique nanoporous structure with a complex pattern of ribs and slits. *K. amoena* is a pennate diatom with bilateral symmetry [34,35]. The silica cell wall, called frustule, is composed of two slightly different valves—the hypotheca (lower part) and the epitheca (upper part), joined together by silica girdle bands (Fig. 1d). Both raphe (Fig. 1c) and rapheless (Fig. 1b) valves are linear and have rostrate ends.

Fig. 2 shows the general cell features and the main terms associated with diatoms. The valve surfaces are ornamented with radiate and parallel striae, represented by a row of pores called areolae. Striae are formed between nonornamented, thickened ribs called costae.

Table 1 summarizes the diatom frustule dimensions. The values presented in the table were obtained from SEM images of ten diatoms with raphe and rapheless valves. The average frustule length in both cases was 9 µm, whereas the average width ranged from 3.7 µm for rapheless valves to 3.9 µm for raphe valves. These dimensions correspond to those of the diatom genus *Karayevia* [34]. The frustule size may differ depending on the generation, medium, and environmental factors such as temperature, light, salinity, and nutrients [36–38].

3.2. DLS measurements

The average size and zeta-potential of the diatom cells were 9 ± 2 µm and −18 ± 6 mV, respectively. There was strong agreement between the results obtained from SEM images and those obtained by

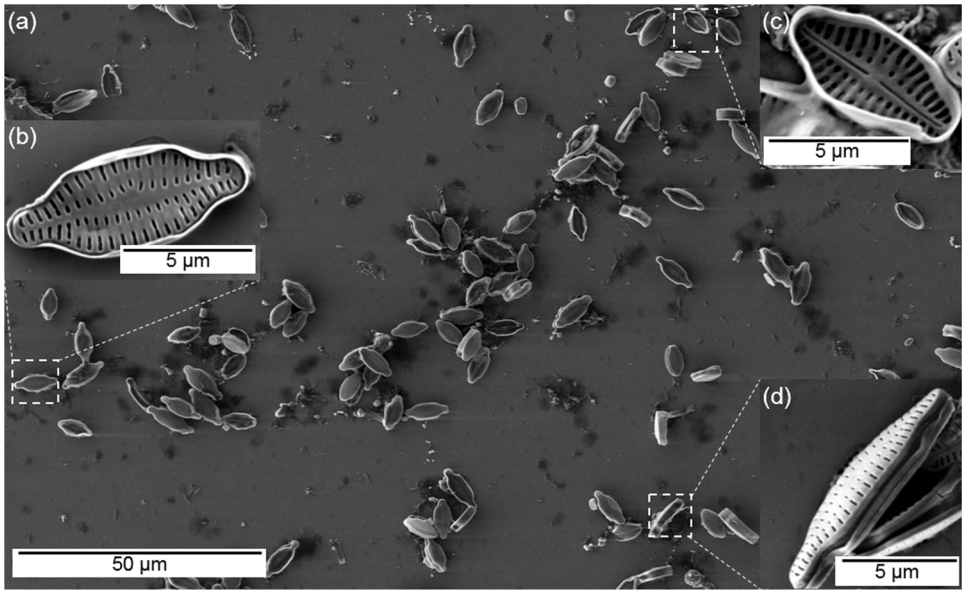

Fig. 1. SEM images of *K. amoena*. (a) overall view. (b) rapheless valve. (c) raphe valve. (d) diatom frustule with girdle bands.

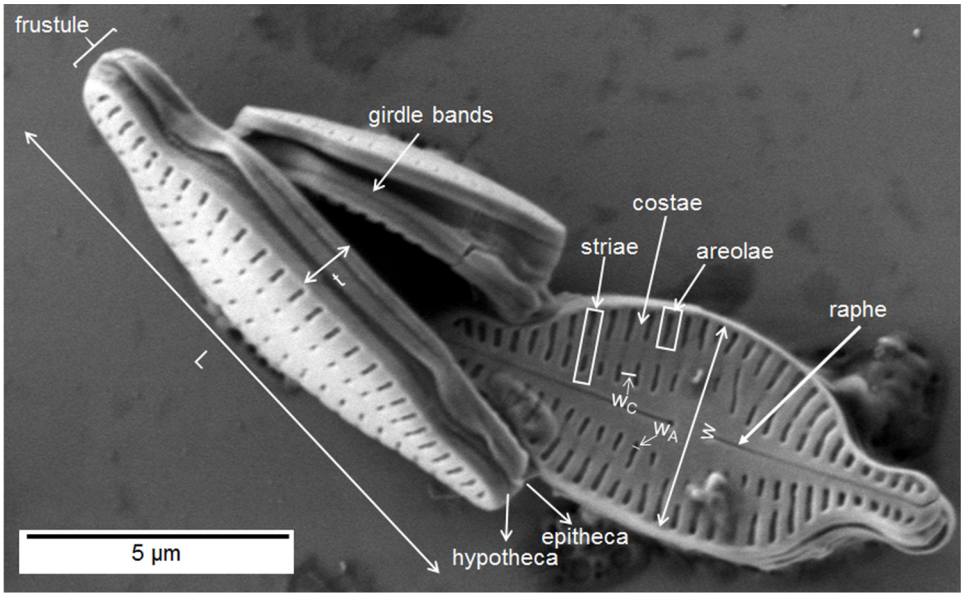

Fig. 2. SEM image of *K. amoena* showing basic cell structure and frustule dimensions: length *L*, width *w*, areola width w_A, costa width w_C, girdle band thickness *t*.

Table 1
Diatom frustule dimensions obtained from SEM images.

Valve	L (μm)	w (μm)	Number of striae per 10 μm	Number of areolae per 10 μm	w_A (μm)	w_C (μm)	t (μm)
Rapheless	9 ± 1	3.7 ± 0.5	23 ± 2	65 ± 4	0.10 ± 0.01	0.36 ± 0.04	1.5 ± 0.2
Raphe	9 ± 2	3.9 ± 0.4	25 ± 4	76 ± 12	0.13 ± 0.02	0.23 ± 0.05	

DLS analysis. The zeta-potential value indicates the beginning of cell agglomeration.

3.3. Fluorescence spectroscopy

Fig. 3 shows the fluorescence spectra of different concentrations of diatoms embedded in agarose gel. The spectra were obtained by excitation at 530 nm wavelength that fits the absorption band for carotenoids. All spectra demonstrate an emission band with a maximum at about 686 nm, which corresponds to chlorophyll *a* [11–15,39,40], and a broad shoulder at 715–740 nm [39,40]. The peak assigned to chlorophyll *a* shifts with decreasing concentration from 686 nm for stock and diluted (1:2, 1:4, and 1:8) suspensions to 680 nm for the most diluted suspension (1:128).

3.4. Absorbance spectroscopy

The absorbance spectra of more concentrated suspensions of diatoms embedded in agarose gel reveal peaks at about 436 nm and 674 nm, attributable to chlorophyll *a* (Fig. 4) [11–15,41–43]. The presence of the carotenoid fucoxanthin is represented by a shoulder at about 500 nm [11–15,41,42]. The band at about 628 nm was assigned

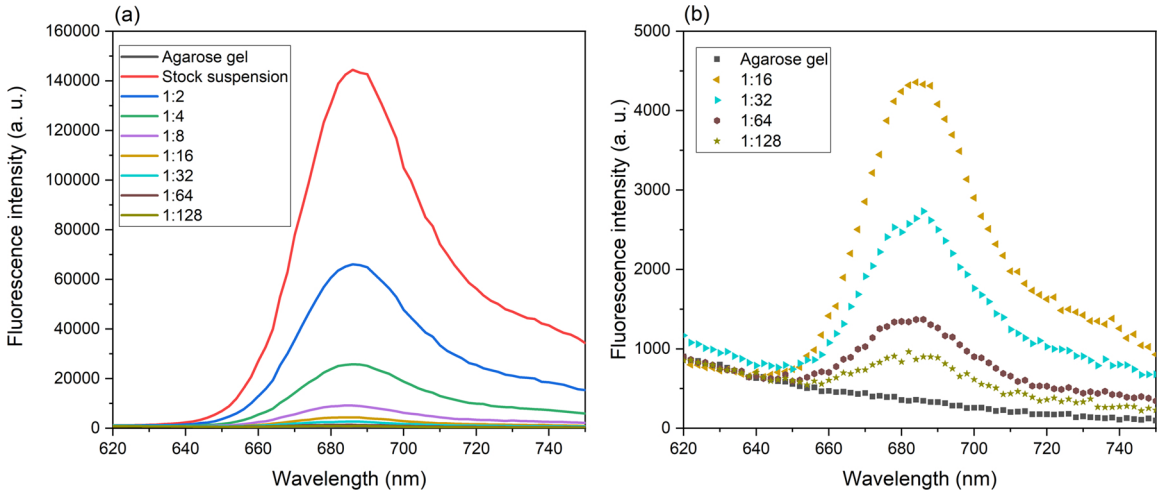

Fig. 3. Fluorescence emission spectra of: (a) different concentrations of *K. amoena* embedded in agarose gel. (b) more diluted suspensions of diatoms mixed with agarose gel. Excitation wavelength: 530 nm.

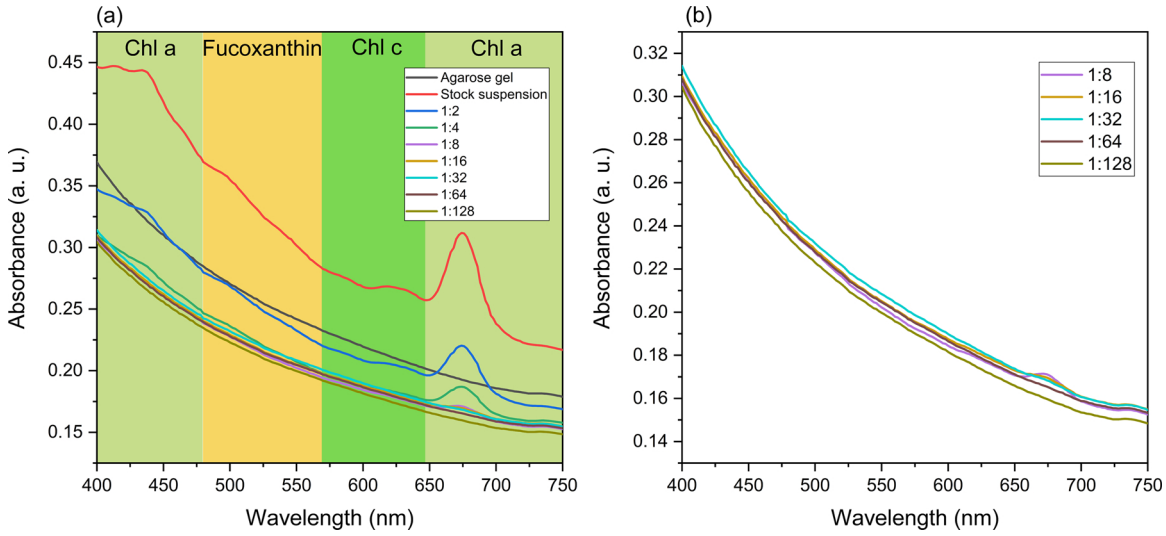

Fig. 4. Absorbance spectra of: (a) different concentrations of *K. amoena* embedded in agarose gel. (b) more diluted suspensions of diatoms mixed with agarose gel. Chl a – chlorophyll *a*, Chl c – chlorophyll *c*.

to chlorophyll *c* [11–15,41,42]. The absorbance was larger for more concentrated suspensions and decreased with decreasing concentration. Only one peak, at 676 nm, was observed for suspensions diluted 1:8 and 1:16. No peaks were observed for suspensions diluted 1:32, 1:64, and 1:128.

3.5. Fluorescence lifetime imaging microscopy measurements

Fig. 5 shows bright-field transmission and fluorescence lifetime images of *K. amoena* diatoms. A strong signal from the diatom stock suspension can be observed. FLIM results demonstrate that diatom chromophores generally have a very short yet changeable average lifetime—from 0.5 to 1 ns (marked in blue to green) to 2 ns (marked in red). The fluorescence signal originated from chlorophyll *a*, because the detection system that was used includes a 638-nm laser as the excitation source and a 690-nm bandpass filter, and it does not record signals other than those from chlorophyll *a*. The system records a variety of chlorophyll lifetimes, probably owing to the complex physiology of diatoms. Another reason could be that in diatoms, pigments have different concentrations, and in some diatoms, they only partly fill the volume of the frustule.

3.6. Photoacoustic measurements

Fig. 6 shows clearly that the photoacoustic signal from *K. amoena* was successfully obtained. The dependence of the photoacoustic signal (represented as the volume of 3D objects) on the diatom concentration shows that the volume of the 3D objects emitting the acoustic signal and the mean pixel intensity increased with the diatom concentration. As shown in Fig. 6e, a low-frequency signal (shown with red bars) is emitted by a greater number of 3D objects than a high-frequency signal (shown with green bars), whereas a high-frequency signal (33–99 MHz) shows a higher mean pixel intensity than a low-frequency signal within the whole concentration range (Fig. 6f).

The interrelation between the volume of diatoms in gel and the volume of 3D objects emitting a photoacoustic signal remains an important issue for discussion in view of the development of fidelity techniques for the quantitative analysis of diatom colonies. The volume of diatoms in an agarose gel drop, V_d, is calculated from the volume of one diatom cell, the concentration of diatom cells c_d, and the volume of agarose gel drop V_{gel} by using Eq. (1):

$$V_d = \frac{4}{3}\cdot\pi\cdot a\cdot b\cdot c\cdot c_d\cdot V_{gel} \quad (1)$$

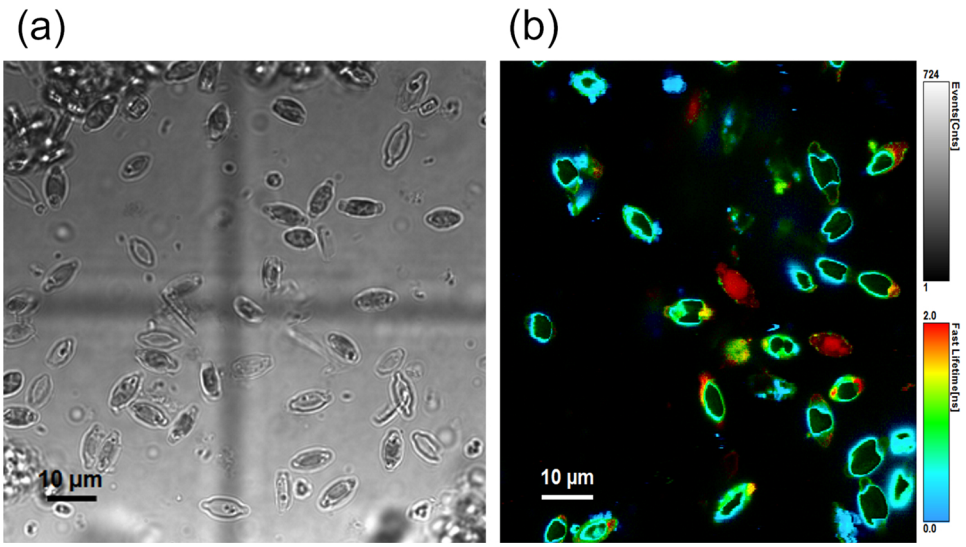

Fig. 5. (a) Transmission bright field and (b) fluorescence lifetime images of *K. amoena*. Excitation wavelength: 638 nm.

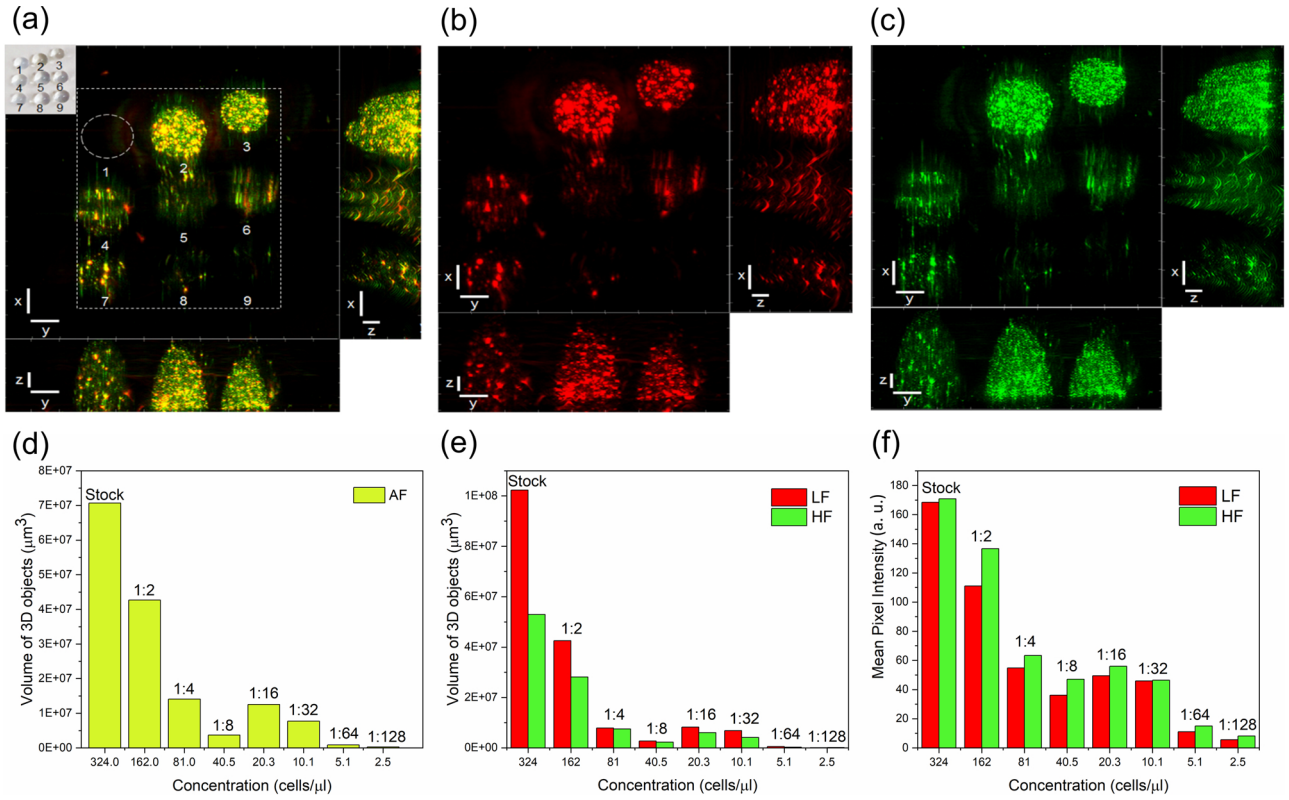

Fig. 6. (a) RSOM image of different concentrations of *K. amoena* embedded in agarose gel at frequencies of 11–99 MHz. Inset: Photograph of different dilutions of *K. amoena* in agarose gel drops, where 1 – Agarose gel; 2 – Stock suspension; Diluted suspensions: 3 - 1:2; 4 – 1:4; 5 – 1:8; 6 – 1:16; 7 – 1:32; 8 – 1:64; 9 – 1:128. (b) RSOM image of *K. amoena* at low frequencies (11–33 MHz). (c) RSOM image of *K. amoena* at high frequencies (33–99 MHz). Scale bar (a,b,c): x-axis – 1 mm, y-axis – 1 mm, z-axis – 0.2 mm. (d) Volume of 3D objects vs. the concentration of diatoms mixed with agarose gel. AF – all frequencies. (e) Volume of 3D objects vs. the concentration of diatoms mixed with agarose gel. LF – low frequencies, HF – high frequencies. (f) Mean pixel intensity vs. the concentration of diatoms mixed with agarose gel.

The diatom cell is approximated as an ellipsoid, where a, b, c are the length, width, and height, respectively. The volume of agarose gel drop V_{gel} is 10 μl.

As one can see from the data in Table 2, there is a wide span of the "volume of 3D objects to the volume of diatoms" ratio for different dilutions of the diatoms in gel.

First of all, the volume of 3D objects is one to two orders of magnitude larger than that of the diatoms. Second, this ratio seems independent of dilution, which hints that the volume of 3D objects is not related to the volume of separate diatom cells but to the volume of cell assemblies containing a number of cells. The resolution of the PA microscope is not high enough to resolve separate diatoms, and the volume of the gel surrounding separate cells is detected as the volume apparently emitting a photoacoustic signal. Another important issue is the nature of the structural element that emits the signal. The chloroplast grains are the obvious candidates; therefore, the distribution and absorption efficiency of the chloroplast grains inside the frustules may contribute to the intensity of the photoacoustic signal.

On the other hand, we believe that the frequencies of acoustic signals emitted by diatoms may correspond to the eigenfrequencies of the natural oscillations of vibrating silica frustules, which can be described as capsular mechanical objects (membrane-shaped shells) having sub- and micrometer sizes [7]. Low frequency modes require less energy for excitation; therefore, even diatoms located deeper in the gel or those partly shadowed receive sufficient energy to excite these low frequencies, ultimately giving rise to 3D objects emitting an acoustic signal. High-frequency vibrations require a higher excitation energy and emit a more intense signal, which varies proportionally to the square of the frequency.

Because the absorbance value for *K. amoena* (Fig. 4) at 532 nm is in agreement with the photoacoustic signal (Fig. 7), we consider chlorophyll *a* and *c* and fucoxanthin as the principal light absorbers responsible for the photoacoustic effect in diatoms, since the 532 nm laser light is absorbed by all of them. A more exact contribution of each chromophore to the detected acoustic signal remains an open question, because it should be examined with two factors in mind:

- The molar absorption coefficient of every chromophore at the wavelength of the laser causing the photoacoustic signal;
- The volume fraction and spatial distribution of the chromophores within the frustule.

It is worth noting that both hemoglobin and chlorophyll, whose photoacoustic behavior is well studied, are complex metal–organic molecules with a central metal atom (Fe and Mg) surrounded by pyrrole

Table 2
Comparison of the volume of 3D objects obtained by using the ImageJ program with the calculated volume of diatom cells in an agarose gel drop.

Dilutions	Volume of 3D objects (ImageJ) / Volume of diatoms in gel (Calculated)
Stock suspension	31
1:2	38
1:4	25
1:8	13
1:16	89
1:32	109
1:64	24
1:128	13

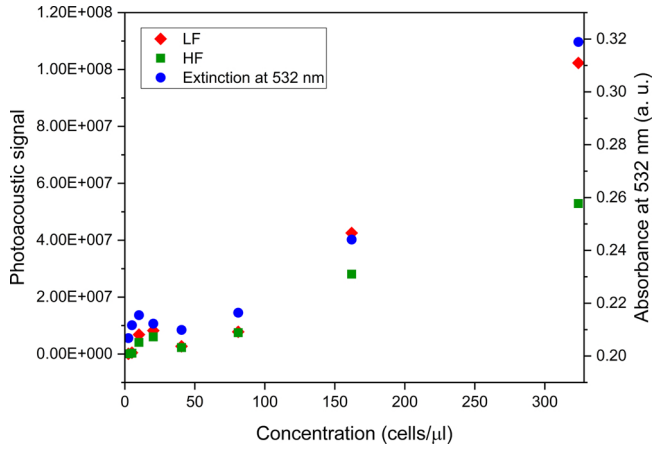

Fig. 7. Dependence of photoacoustic signal and absorbance at 532 nm on concentration of diatoms mixed with agarose gel. LF – low frequencies, HF – high frequencies.

rings [44]. Fucoxanthin does not contain pyrrole rings, which supports the suggestion that chlorophyll has a leading role in the formation of a photoacoustic signal.

Photoacoustic visualization of human tissues and cells and thermal (plasmonic) heating *in situ* have been proposed for use in medical diagnostics and therapy. The application of photoacoustics to bacteria, algae, and other nonhuman natural objects is a relatively undeveloped area that leaves lacunae of knowledge and unexplored opportunities in biotechnology. We report the successful photoacoustic visualization of single-cell algal organisms—diatoms. Considering the significant role of diatoms in Earth's biosphere, we suppose that our findings may pave the way to a number of applications mainly related to the rapid probing of sea, fresh, and waste water, in which the diatom concentration reflects the ecological well-being and the productivity of biomass. Recent advances in diatom biofuel [45], aquaculture [46], and the management of plastic waste in the world ocean [47] suggest that the use of rapid and remote monitoring systems based on the photoacoustic effect may find interesting applications.

We believe that PA methods are particularly suitable for use in bioreactors or aquaculture installations for the fast detection and gentle *in situ* evaluation of the density of diatom colonies formed from relatively small cells (9 ± 1 μm) such as *K. amoena*. Owing to the presence of chromophores, these methods are sensitive to the organic content of diatoms and do not require sophisticated sample preparation. Separate cells of *K. amoena* are not resolved because of the instrumental limitations, whereas diatom clusters and colonies are clearly visualized, which is of utmost importance for aquaculture monitoring. Moreover, large individual diatom cells (e.g. *Ethmodiscus* or *Synedra*, which are larger than 200 μm) seem ready for visualization. This successful demonstration of the working principle of photoacoustics for the visualization of diatom colonies promises further developments toward the PA imaging of individual cells. The fundamental cell studies related to the careful continuous characterization of algal colonies could be substantially improved, facilitated, automated, and simplified if supported by large 3D probes. Chromophore-containing symbiotic bacteria, such as some components of the stomach flora [48] or plunge bacteria, should be considered for use in further work.

4. Conclusions

Photoacoustic visualization, widely used in the diagnostics and studies of tissues, organs, and cells of mammals, was successfully tested to characterize a single-celled organism—the pennate diatom *K. amoena*. Being natural photosynthesizers, diatom algae contain significant amounts of the chromophores—chlorophyll and fucoxanthin—and, therefore, exhibit a strong photoacoustic effect, excited by a green, 532-nm laser. This allows the visualization and quantitative study of diatom colonies in natural media without complex sample preparation procedures, such as those required in light and scanning electron microscopy. The intensity of the photoacoustic signal, with the main contribution from the low-frequency portion (11–33 MHz), increases with the diatom concentration within the probed volume, which ensures reliable calibration for rapid tests. The findings from this study could be applied in the remote and rapid automated monitoring of the ecological well-being of open water bodies.

Funding

The culturing of the diatoms was funded in part under Russian Foundation for Basic Research (RFBR) grant no. 18-44-920012.

Declaration of Competing Interest

The authors declare that there are no conflicts of interest.

Acknowledgments

We express our gratitude to Maksim Mokrousov and Olga Gusliakova for their assistance in DLS and absorbance measurements and for the support provided under Russian Foundation for Basic Research grant no. 18-44-920012. Alexander M. Korsunsky acknowledges support from the Royal Society of London through grant no. IEC/R2/170223, which enabled a range of collaborations leading to the results reported in this paper. Marina V. Novoselova thanks the Russian Science Foundation (grant no. 18-73-00307) for support toward RSOM studies. We are especially thankful to Yaroslava V. Kalyaeva for her fruitful research and constructive contribution to the development of diatom culturing procedures. Authors thank Advanced Imaging Core facility of Skolkovo Institute of Science and Technology for valuable support in SEM imaging and studies.

Appendix A. Supplementary data

Supplementary material related to this article can be found, in the online version, at doi:https://doi.org/10.1016/j.pacs.2020.100171.

References

[1] C. Li, L.V. Wang, Photoacoustic tomography and sensing in biomedicine, Phys. Med. Biol. 54 (2009), https://doi.org/10.1088/0031-9155/54/19/R01.
[2] R.O. Esenaliev, Optoacoustic diagnostic modality: from idea to clinical studies with highly compact laser diode-based systems, J. Biomed. Opt. 22 (2017) 091512–091518, https://doi.org/10.1117/1.jbo.22.9.091512.
[3] R.O. Esenaliev, A.A. Karabutov, A.A. Oraevsky, Sensitivity of laser opto-acoustic imaging in detection of small deeply embedded tumors, IEEE J. Sel. Top. Quantum Electron. 5 (1999) 981–988, https://doi.org/10.1109/2944.796320.
[4] L.V. Wang, S. Hu, Photoacoustic tomography: in vivo imaging from organelles to organs, Science 335 (2012) 1458–1462, https://doi.org/10.1126/science.1216210 T5A.1.
[5] R.O. Esenaliev, Optoacoustic monitoring of physiologic variables, Front. Physiol. 8 (2017) 1–6, https://doi.org/10.3389/fphys.2017.01030.
[6] A.M. Korsunsky, A.I. Salimon, On the paradigm of hierarchically structured materials, in conjunction with the virtual special issue on functional materials, Mater. Des. 158 (2018) 1–4, https://doi.org/10.1016/j.matdes.2018.08.008.
[7] B. Abdusatorov, J. Everaerts, A.I. Salimon, A.M. Korsunsky, On the prospects of using Biogenic Silica for MEMS (Micro-Electro-Mechanical Systems), Proceedings of the World Congress on Engineering 2019, WCE 2019, July 3–5, 2019, London, U.K., 2019.
[8] F.R. Lamastra, M.L. Grilli, G. Leahu, A. Belardini, R. Li Voti, C. Sibilia, D. Salvatori, I. Cacciotti, F. Nanni, Diatom frustules decorated with zinc oxide nanoparticles for enhanced optical properties, Nanotechnology 28 (2017), https://doi.org/10.1088/1361-6528/aa7d6f.
[9] F.R. Lamastra, M.L. Grilli, G. Leahu, A. Belardini, R. Li Voti, C. Sibilia, D. Salvatori, I. Cacciotti, F. Nanni, Photoacoustic spectroscopy investigation of zinc oxide/diatom frustules hybrid powders, Int. J. Thermophys. 39 (2018) 1–10, https://doi.org/10.1007/s10765-018-2428-6.
[10] Z. Dubinsky, J. Feitelson, D.C. Mauzerall, Listening to phytoplankton: measuring

biomass and photosynthesis by photoacoustics, J. Phycol. 34 (1998) 888–892, https://doi.org/10.1046/j.1529-8817.1998.340888.x.
[11] J.S. Brown, Photosynthetic pigment organization in diatoms (Bacillariophyceae), J. Phycol. 24 (1988) 96–102, https://doi.org/10.1111/j.1529-8817.1988.tb04460.x.
[12] P. Kuczynska, M. Jemiola-Rzeminska, K. Strzalka, Photosynthetic pigments in diatoms, Mar. Drugs 13 (2015) 5847–5881, https://doi.org/10.3390/md13095847.
[13] S. Akimoto, A. Teshigahara, M. Yokono, M. Mimuro, R. Nagao, T. Tomo, Excitation relaxation dynamics and energy transfer in fucoxanthin- chlorophyll a/c-protein complexes, probed by time-resolved fluorescence, Biochim. Biophys. Acta - Bioenergy 1837 (2014) 1514–1521, https://doi.org/10.1016/j.bbabio.2014.02.002.
[14] D.F. Millie, O.M.E. Schofield, G.J. Kirkpatrick, G. Johnsen, T.J. Evens, Using absorbance and fluorescence spectra to discriminate microalgae, Eur. J. Phycol. 37 (2002) 313–322, https://doi.org/10.1017/S0967026202003700.
[15] A. Burson, M. Stomp, E. Greenwell, J. Grosse, J. Huisman, Competition for nutrients and light: testing advances in resource competition with a natural phytoplankton community, Ecology 99 (2018) 1108–1118, https://doi.org/10.1002/ecy.2187.
[16] W. Becker, Fluorescence lifetime imaging - techniques and applications, J. Microsc. 247 (2012) 119–136, https://doi.org/10.1111/j.1365-2818.2012.03618.x.
[17] D. Elson, S. Webb, J. Siegel, K. Suhling, D. Davis, J. Lever, D. Phillips, A. Wallace, P. French, Biomedical applications of fluorescence lifetime imaging, Opt. Photonics News 13 (2002) 26–32, https://doi.org/10.1364/opn.13.11.000026.
[18] L.C. Chen, W.R. Lloyd, C.W. Chang, D. Sud, M.A. Mycek, Fluorescence Lifetime Imaging Microscopy for Quantitative Biological Imaging, 4th ed., Elsevier Inc., 2013, https://doi.org/10.1016/B978-0-12-407761-4.00020-8.
[19] J. Korczyński, J. Włodarczyk, Fluorescence lifetime imaging microscopy (FLIM) in biological and medical research, Postepy Biochem. 55 (2009) 434–440 http://www.ncbi.nlm.nih.gov/pubmed/20201357.
[20] P.G. Falkowski, H. Lin, M.Y. Gorbunov, What limits photosynthetic energy conversion efficiency in nature? Lessons from the oceans, Philos. Trans. R. Soc. B Biol. Sci. 372 (2017) 2–8, https://doi.org/10.1098/rstb.2016.0376.
[21] J. Lavaud, B. Lepetit, An explanation for the inter-species variability of the photoprotective non-photochemical chlorophyll fluorescence quenching in diatoms, Biochim. Biophys. Acta – Bioenergy 1827 (2013) 294–302, https://doi.org/10.1016/j.bbabio.2012.11.012.
[22] A.M. Korsunsky, P.V. Sapozhnikov, J. Everaerts, A.I. Salimon, Nature's neat nanostructuration: the fascinating frustules of diatom algae, Mater. Today 22 (2019) 159–160, https://doi.org/10.1016/j.mattod.2019.01.002.
[23] K. Verma, Role of diatoms in the world of forensic science, J. Forensic Res. 4 (2013) 2–5, https://doi.org/10.4172/2157-7145.1000181.
[24] Z. Levkov, D.M. Williams, D. Nikolovska, S. Tofilovska, Z. Cakar, The use of diatoms in forensic science: advantages and limitations of the diatom test in cases of drowning, Archaeol. Forensic Appl. Microfossils A Deep. Underst. Hum. Hist. (2017), pp. 261–277, https://doi.org/10.1144/tms7.14.
[25] I. Ruggiero, M. Terracciano, N.M. Martucci, L. De Stefano, N. Migliaccio, R. Tatè, I. Rendina, P. Arcari, A. Lamberti, I. Rea, Diatomite silica nanoparticles for drug delivery, Nanoscale Res. Lett. 9 (2014) 1–7, https://doi.org/10.1186/1556-276X-9-329.
[26] D. Losic, Y. Yu, M.S. Aw, S. Simovic, B. Thierry, J. Addai-Mensah, Surface functionalisation of diatoms with dopamine modified iron-oxide nanoparticles: toward magnetically guided drug microcarriers with biologically derived morphologies, Chem. Commun. 46 (2010) 6323–6325, https://doi.org/10.1039/c0cc01305f.
[27] M.S. Aw, S. Simovic, J. Addai-Mensah, D. Losic, Silica microcapsules from diatoms as new carrier for delivery of therapeutics, Nanomedicine (Lond) 6 (2011) 1159–1173, https://doi.org/10.2217/nnm.11.29.
[28] B. Delalat, V.C. Sheppard, S. Rasi Ghaemi, S. Rao, C.A. Prestidge, G. McPhee, M.L. Rogers, J.F. Donoghue, V. Pillay, T.G. Johns, N. Kröger, N.H. Voelcker, Targeted drug delivery using genetically engineered diatom biosilica, Nat. Commun. 6 (8791) (2015) 1–11, https://doi.org/10.1038/ncomms9791.
[29] M. Milović, S. Simović, D. Lošić, A. Dashevskiy, S. Ibrić, Solid self-emulsifying phospholipid suspension (SSEPS) with diatom as a drug carrier, Eur. J. Pharm. Sci. 63 (2014) 226–232, https://doi.org/10.1016/J.EJPS.2014.07.010.
[30] J. Janićijević, D. Krajišnik, B. Čalija, B.N. Vasiljević, V. Dobričić, A. Daković, M.D. Antonijević, J. Milić, Modified local diatomite as potential functional drug carrier - a model study for diclofenac sodium, Int. J. Pharm. 496 (2015) 466–474, https://doi.org/10.1016/j.ijpharm.2015.10.047.
[31] R. Ragni, S. Cicco, D. Vona, G. Leone, G.M. Farinola, Biosilica from diatoms microalgae: smart materials from bio-medicine to photonics, J. Mater. Res. 32 (2017) 279–291, https://doi.org/10.1557/jmr.2016.459.
[32] Karayevia amoena | Species - Diatoms of North America, Diatoms.Org. https://diatoms.org/species/karayevia_amoena (Accessed 5 January 2020).
[33] M.D. Mokrousov, M.V. Novoselova, J. Nolan, W. Harrington, P. Rudakovskaya, D.N. Bratashov, E.I. Galanzha, J.P. Fuenzalida-Werner, B.P. Yakimov, G. Nazarikov, V.P. Drachev, E.A. Shirshin, V. Ntziachristos, A.C. Stiel, V.P. Zharov, D.A. Gorin, Amplification of photoacoustic effect in bimodal polymer particles by self-quenching of indocyanine green, Biomed. Opt. Express 10 (2019) 4775–4789, https://doi.org/10.1364/boe.10.004775.
[34] L. Bukhtiyarova, Additional data on the diatom genus *Karayevia* and a proposal to reject the genus Kolbesia, Nov. Hedwigia Beih. 130 (2006) 85–96.
[35] F.E. Round, L. Bukhtiyarova, Four new genera based on achnanthes (achnanthidium) together with a re-definition of achnanthidium, Diatom Res. 11 (1996) 345–361, https://doi.org/10.1080/0269249X.1996.9705389.
[36] Z.V. Finkel, C.J. Vaillancourt, A.J. Irwin, E.D. Reavie, J.P. Smol, Environmental control of diatom community size structure varies across aquatic ecosystems, Proc. R. Soc. B Biol. Sci. 276 (2009) 1627–1634, https://doi.org/10.1098/rspb.2008.1610.
[37] E. Litchman, C.A. Klausmeier, K. Yoshiyama, Contrasting size evolution in marine and freshwater diatoms, Proc. Natl. Acad. Sci. U. S. A. 106 (2009) 2665–2670, https://doi.org/10.1073/pnas.0810891106.
[38] F. Svensson, J. Norberg, P. Snoeijs, Diatom cell size, coloniality and motility: trade-offs between temperature, salinity and nutrient supply with climate change, PLoS One 9 (2014) 1–17, https://doi.org/10.1371/journal.pone.0109993.
[39] K. Sugahara, N. Murata, Fluorescence of chlorophyll in brown algae and diatoms, Plant Cell Physiol. 385 (1971) 377–385, https://doi.org/10.1093/oxfordjournals.pcp.a074631.
[40] J.S. Brown, The fluorescence emission spectra of chlorophyll a forms from euglena, Biochim. Biophys. Acta - Biophys. Incl. Photosynth. 120 (1966) 305–307, https://doi.org/10.1016/0926-6585(66)90352-9.
[41] R. Aguirre-Gómez, A.R. Weeks, S.R. Boxall, The identification of phytoplankton pigments from absorption spectra, Int. J. Remote Sens. 22 (2001) 315–338, https://doi.org/10.1080/014311601449952.
[42] R.J. Geider, B.A. Osborne, Light absorption by a marine diatom: experimental observations and theoretical calculations of the package effect in a small Thalassiosira species, Mar. Biol. 96 (1987) 299–308, https://doi.org/10.1007/BF00427030.
[43] V. Stuart, S. Sathyendranath, E.J.H. Head, T. Platt, B. Irwin, H. Maass, Bio-optical characteristics of diatom and prymnesiophyte populations in the Labrador Sea, Mar. Ecol. Prog. Ser. 201 (2000) 91–106, https://doi.org/10.3354/meps201091.
[44] P. Rothemund, Hemin and chlorophyll: the two most important pigments for life on Earth, Ohio J. Sci. 56 (1956) 193–202.
[45] J.K. Wang, M. Seibert, Prospects for commercial production of diatoms, Biotechnol. Biofuels 10 (2017) 1–13, https://doi.org/10.1186/s13068-017-0699-y.
[46] X.L. Li, T.K. Marella, L. Tao, L. Peng, C.F. Song, L.L. Dai, A. Tiwari, G. Li, A novel growth method for diatom algae in aquaculture waste water for natural food development and nutrient removal, Water Sci. Technol. 75 (2017) 2777–2783, https://doi.org/10.2166/wst.2017.156.
[47] A.I. Salimon, J. Everaerts, P.V. Sapozhnikov, E.S. Statnik, M. Alexander, On diatom colonization of porous UHMWPE scaffolds, Proceedings of the World Congress on Engineering 2018 Vol II WCE 2018, July 4–6, 2018, London, U.K., 2018.
[48] X. Huang, Y. Shi, Y. Liu, H. Xu, Y. Liu, C. Xiao, J. Ren, L. Nie, Noninvasive photoacoustic identification and imaging of gut microbes, Opt. Lett. 42 (2017) 2938–2940, https://doi.org/10.1364/ol.42.002938.

Julijana Cvjetinovic received her B.S. in Physics from University of Novi Sad, Serbia and her M.S. in Condensed Matter Physics from National University of Science and Technology "MISiS", Moscow, Russia. She is currently a PhD student at the Center for Photonics and Quantum Materials at Skolkovo Institute of Science and Technology. During her Master's degree studies she worked on development of hybrid materials based on natural and synthetic polymers for reconstructive surgery. Her current research is focused on using different photonic and bioimaging techniques to study composite multifunctional nanostructured particles based on the mineral shells of unicellular algae for applications in medicine and dentistry.

Alexey I. Salimon, studied Physics of Metals and received his MSc and PhD degree in NUST «MISIS» Moscow, Russia working on structure change in metals under severe plastic deformation. For more than 20 years he works in the field of new and smart materials and technologies: nanostructured metals and alloys, quasicrystalline intermetallics, bulk metal glasses, composites, elastomers resistant to explosion decompression, and recently bio-derived materials. Post-doc researcher in 1997–1998 in Newcastle University, UK in the group of Professor Korsunsky and in 2002–2004 in INPG (Grenoble, France) together with Professors M.F. Ashby and Y. Brechet. For more than 12 years Dr Salimon as R&D specialist worked in industry for companies supplying oil&gas equipment and high performance parts.

Marina Novoselova is the Research Scientist at the Biophotonic laboratory, Skolkovo Institute of Science and Technologies. She received the Ph.D. in engineering science (2016). Marina Novoselova has more than 6 years of research experience in the fields of bionanotechnology and material sciences. Her current interests are targeted therapeutics and magnetic drug delivery and developing of contrast agents for fluorescent and photoacoustic imaging.

Dr. Philip Sapozhnikov received his Ph.D. in hydrobiology at the P.P. Shirshov Institute of Oceanology of RAS, Russia, in 2010. He studied at Lomonosov Moscow State University in the period from 1993 to 1998. Received a specialist diploma at the Department of Algology and Mycology. In 1996 he began working at the P.P. Shirshov Institute of Oceanology of RAS, in the laboratory of ecology of coastal bottom communities, currently - as a senior researcher. His specialization: ecology and forms of self-organization of communities of bottom microorganisms that can metamorphize the environment. A separate deep attention in his scientific work is devoted to diatoms: their ecology, forms of reproduction, movement strategies, self-organization of communities: both in nature and in experimental conditions.

Dr. Evgeny Shirshin received his PhD in 2011 from the Lomonosov Moscow State University, Russia, in the field of laser spectroscopy. He is currently working as a senior research scientist in Lomonosov Moscow State University and is the head of the Laser biophotonics laboratory. The research of E. Shirshin is focused on molecular imaging with endogenous contrast for biomedical diagnostics and fundamental aspects of optical properties formation in heterogenous systems.

Dr. Alexey Yashchenok obtained his PhD degree in Physics from Saratov State University, Russia in 2007. He stayed at the Max-Planck Institute of Colloids and Interfaces (Potsdam-Golm, Germany) from 2010 to 2014, where he studied remote opening of microcontainers, cell behaviour and organization of metallic nanoparticles to achieve ultrasensitive fluorescence and Raman detection of metabolites inside a cell. He completed his habilitation in Biophysics in 2017 at Saratov State University. He joined Center for Photonics and Quantum Materials at Skoltech as leading research scientist in 2017. His work is focused on biophysics, synthesis and self-assembly of multifunctional stimuli responsive nanostructured materials for sensing, drug delivery and therapy, fluorescent and Raman microscopy, diagnostic and imaging methods for biomedical applications.

Dr. Olga Kalinina studied at the Pedagogical Institute of the city of Kurgan, Russia, from 1987 to 1992, and received a teacher's diploma in biology and chemistry. From 2010 to the present, she works in the laboratory of renewable energy sources of the Geography Faculty of Lomonosov Moscow State University. Now holds the position of junior research assistant. From 2012 to the present, she works in the laboratory of ecology of coastal bottom communities P.P. Shirshov Institute of Oceanology of RAS. Her scientific specialization is the cultivation of highly productive microalgae cultures, including diatoms and cyanobacteria, in order to obtain strains suitable for the production of a large number of unsaturated fatty acids as raw materials for biodiesel.

Professor Alexander Korsunsky is a world-leader in engineering microscopy of materials for optimisation of design, durability and performance. He leads the MBLEM lab (Multi-Beam Laboratory for Engineering Microscopy) at Oxford, and the Centre for In situ Processing Science at the Research Complex, Harwell. He consults Rolls-Royce plc on matters of residual stress and structural integrity, and is Editor-in Chief of Materials & Design, a major Elsevier journal (2018 impact factor 5.770). Alexander holds the degree of Doctor of Philosophy (DPhil) from Merton College, Oxford. Prof Korsunsky's research interests concern improved understanding of integrity and reliability of engineered and natural structures and systems, from high-performance metallic alloys to polycrystalline ceramics to natural hard tissue such as human dentin and seashell nacre.

Dmitry Gorin is a professor at the Skoltech center of Photonics & Quantum Materials (Moscow, Russia) and head of Biophotonics Lab. He has received Diploma of Engineer-Physicist (Specialty: Materials and Components of Solid-State Electronics) in 1997 and his PhD degree and his DSc degree in Physical Chemistry in 2001 and 2011 from Saratov State University, respectively. He was a PostDoc fellow in the Max Planck Institute of Colloids and Interfaces from 2009 till 2010. He was professor at Department of Nano- and Biomedical Technologies at Saratov State University from 2011 till 2017. In 2017 he was awarded Professor in a specialty Biophysics by VAK. Research interests of Prof. Gorin are in Biophysics, Biophotonics, Theranostics, Physics and Chemistry of Colloids and Interfaces.